Electrochimica Acta 425 (2022) 140690

Contents lists available at ScienceDirect

Electrochimica Acta

journal homepage: www.journals.elsevier.com/electrochimica-acta

Antimony nanomaterials modified screen-printed electrodes for the voltammetric determination of metal ions

María A. Tapia [a], Clara Pérez-Ràfols [a,b], Jan Paštika [c,*], Rui Gusmão [c,*], Núria Serrano [a,b,**], Zdeněk Sofer [c], José Manuel Díaz-Cruz [a,b]

[a] Department of Chemical Engineering and Analytical Chemistry, University of Barcelona (UB), Martí i Franquès 1-11, Barcelona 08028, Spain
[b] Water Research Institute (IdRA), University of Barcelona, Martí i Franquès 1-11, Barcelona 08028, Spain
[c] Department of Inorganic Chemistry, University of Chemistry and Technology Prague, Technicka 5, Prague 6, 166 28, Czech Republic

ARTICLE INFO

Keywords:
Antimonene
Antimony chalcogenide
Layered materials
Screen-printed electrodes
Stripping voltammetry

ABSTRACT

Exfoliated β-Sb or two dimensional (2D) antimonene-based modified screen-printed electrode (2D Sb-SPCE), prepared by drop-casting of an exfoliated layered β-antimony (2D Sb) suspension, was used for the simultaneous determination of Pb(II) and Cd(II) by differential pulse anodic stripping voltammetry (DPASV). 2D Sb-SPCE was characterized by microscopic and analytical techniques, and compared not only to bare SPCE but also to layered antimony chalcogenides based-sensors. Both Sb_2S_3 and Sb_2Se_3 have an isomorphous tubular one-dimensional (1D) crystal structure, whereas Sb_2Te_3 and monoelement β-Sb have a 2D layered structure. Under optimized conditions, 2D Sb-SPCE displays an excellent analytical performance with detection limits of 0.3 and 2.7 μg L^{-1} for Pb(II) and Cd(II), respectively, and a linear response from 1.1 to 128.3 μg L^{-1} for Pb(II) and from 9.1 to 132.7 μg L^{-1} for Cd(II). Moreover, 2D Sb-SPCE was successfully applied for the DPASV determination of Pb(II) and Cd (II) in tap water, achieving statistically comparable results to those provided by ICP-MS measurements.

1. Introduction

Stripping analysis is a well-known and suited technique for the analytical determination of trace metal ions due to its high sensitivity, low limits of detection and relatively low instrumentation and maintenance economical cost [1,2]. A key aspect in its analytical performance is the chemical nature of the working electrode, which should ensure an effective preconcentration and redox reaction of the target compound, a highly reproducible and easily renewable electrode surface and a wide potential window in the cathodic region [3]. In this context, working electrodes based on bismuth and antimony have proven to provide a comparable analytical performance to mercury electrodes, revealing the chemical elements in group 15 of the periodic table (also known as Group VA or pnictogens) as a great choice for the development of effective and reliable working electrodes for stripping measurements [3–6]. Several types of bismuth and antimony electrodes are found in the literature, including metal films (both *in-situ* and *ex-situ*), bulk, sputtered, and doped electrodes [5,6].

The rise of 2D layered materials following the great success of graphene has introduced new possibilities for the development of electrochemical sensors due to their high surface area, morphology tunability, excellent mobility, and the possibility of altering their surface properties [7–9]. Indeed, several inorganic layered materials have been reported to manifest a superior performance over their bulk counterparts [8–10]. In this context, both bismuth and antimony may be developed in a 2D layer structure, typically in a rhombohedral arrangement [9]. However, although the implementation of bismuthene and antimonene as voltammetric sensors presents a great potential, scarce literature is found on the subject [11]. Our group recently reported an exfoliated layered bismuth (2D Bi) based screen-printed electrode (SPE) for the stripping determination of cadmium(II) and lead(II), which demonstrated a superior analytical performance than typical bismuth-based electrodes by providing limits of detection as low as 0.06 and 0.07 μg L^{-1} for Pb(II) and Cd(II), respectively [12]. Similar results were also reported by Lazanas et al. [13]. All this suggests that a similar outcome is expected for exfoliated layered antimony (2D Sb), with the associated

* Corresponding author at: Department of Inorganic Chemistry, University of Chemistry and Technology Prague, Technicka 5, Prague 6, 166 28, Czech Republic.
** Corresponding author at: Department of Chemical Engineering and Analytical Chemistry, University of Barcelona, Martí i Franquès 1-11, Barcelona 08028, Spain.
E-mail addresses: rui.gusmao@vscht.cz (R. Gusmão), nuria.serrano@ub.edu (N. Serrano).

https://doi.org/10.1016/j.electacta.2022.140690
Received 26 April 2022; Received in revised form 27 May 2022; Accepted 7 June 2022
Available online 7 June 2022
0013-4686/© 2022 The Author(s). Published by Elsevier Ltd. This is an open access article under the CC BY license (http://creativecommons.org/licenses/by/4.0/).

electrochemical and analytical benefits of antimony electrodes as compared to bismuth-based electrodes (e.g., wider potential window, and capability of working in acidic solutions [5]).

The 2D layered gray, β-phase or rhombohedral arsenic, antimony, and bismuth occur naturally, thus being the most commonly used in research [11]. Similarly, antimony chalcogenides Sb_2X_3 (X = S, Se, or Te) have also emerged as nontoxic, highly stable, and low-cost layered materials [14,15]. Both Sb_2S_3 and Sb_2Se_3 have an isomorphous tubular one-dimensional (1D) crystal structure and are found in nature as the crystalline mineral stibnite and antimonselite, respectively. Rhombohedral Sb_2Te_3 has a 2D layered structure, is a narrow-gap semiconductor, also designated as a topological insulator, and has thickness-dependent physical properties.

A few recent works have explored the implementation of 2D Sb in the development of electrochemical (bio)sensors for the determination of H_2O_2 [16], 4-nitrotoluene [17], phenol [18], and BRCA1 gene [19], among others. However, despite the excellent features attributed to antimony based- electrodes and the outperformance exhibited by inorganic layered materials, to the best of our knowledge the possibilities of 2D Sb or the corresponding layered antimony chalcogenides as sensing materials in the stripping voltammetric determination of trace metal ions have not been explored yet.

Thus, this work presents a 2D Sb modified screen-printed carbon electrode (2D Sb-SPCE) for the anodic stripping voltammetric determination of cadmium(II) and lead(II) as a model system for trace metal ion determination. The developed sensor presents an enhanced electrochemical and analytical performance as compared to the bare SPCE and is a much better suited option than the corresponding layered antimony chalcogenides. The presented 2D Sb-SPCE was also tested for the analysis of real samples, demonstrating its ability to accurately determine cadmium(II) and lead(II) even in samples with complex matrix.

2. Experimental section

2.1. Chemicals and solutions

Suprapur grade hydrochloric acid (30%), acetic acid and sodium acetate trihydrate (analytical grade) were purchased from Merck (Darmstadt, Germany). Isopropanol was purchased from VWR chemicals (Darmstadt, Germany). Gray antimony, sulfur, selenium, and tellurium granules of 5 N purity were acquired from STREM.

Diluted working solutions were daily prepared from 0.01 mol L^{-1} standard stock solutions of Pb(II) and Cd(II) previously standardized by complexometric titration.

Tap water sample was collected from the local water distribution network, managed by Agbar Company (Barcelona; https://www.agbar.es/), and mostly coming from Llobregat river. The sample was fortified with Pb(II) and Cd(II) at concentrations levels of 160.5 μg L^{-1} and 111.7 μg L^{-1}, respectively. The sample was acidified to pH 2 with HCl and stored in the refrigerator.

All solutions were prepared using ultrapure water (18.4 MΩ cm) obtained from a Milli-Q reference $A+$ water purification system (Millipore, France).

2.2. Instrumentation and procedures

2.2.1. Synthesis of antimony chalcogenides

Antimony chalcogenides were prepared by direct reaction of element and chalcogenide in a quartz glass ampoule under high vacuum. The quartz glass ampoule (25×100 mm) was filled with stoichiometric amounts of antimony and chalcogenide corresponding to 10 g of antimony chalcogenide with accuracy better than 0.5 mg. The ampoule was evacuated on the base pressure of 10^{-3} Pa and melt sealed by oxygen-hydrogen welding torch. The ampoule was placed horizontally in a muffle furnace and heated to 700 °C using a heating rate of 5 °C min^{-1}. The ampoule was held at this temperature for 5 h and then cooled to room temperature using a cooling rate of 1 °C min^{-1}. Finally, the formed crystals of antimony chalcogenide were mechanically removed from the ampoule and shortly grinded in an agate mortar, obtaining the powder that will be used as starting material for further exfoliation.

2.2.2. Shear force exfoliation

The exfoliating method for Sb, Sb_2S_3, Sb_2Se_3 and Sb_2Te_3 was adapted from a previously reported method [12,20]. Briefly, 0.5–1.0 g of the selected material were dispersed in 120 mL of 1:1 isopropanol:water solution. The obtained dispersion was then submitted to shear force exfoliation by means of a T 18 digital Ultra-Turrax instrument (IKA, Wiesenweg, Germany) with a dispersion stainless-steel foot S18N-19 G, at 20 krpm for 90 min. The exfoliating procedure was conducted under N_2 atmosphere and cooled by means of an ice bath to prevent the solution from overheating.

The obtained suspension was centrifuged at 1.5 krpm for 10 min, and then filtered with a 0.20 μm pore size, 4.7 cm diameter nylon filter. The resulting material was dried in the oven at 25 °C overnight and stored under vacuum until further use.

2.2.3. Characterization of materials

Scanning electron microscopy (SEM), combined with energy-dispersive X-ray spectroscopy (EDXS) measurements were conducted at an acceleration voltage of 20 kV. Bulk materials powder were placed on top of carbon tape. Elemental composition was investigated by EDXS using an X-Max^N detector from Oxford Instruments. Transmission electron microscopy (TEM) images were obtained using EFTEM Joel 2200 FS microscope. Samples were prepared by drop casting of each material suspension (0.5 mg/mL) on a 200 mesh TEM grid. Elemental maps were enquired with SDD detector X-MaxN 80 T S from Oxford Instruments (England), at 200 kV.

2.2.4. Preparation of modified SPEs

Individual modifier suspensions at several concentration values were prepared from 2D Sb, Sb_2S_3, Sb_2Se_3 and Sb_2Te_3. For 2D Sb, the concentrations of the considered modifier suspensions were 0.75, 1.12, 2.50, and 5.00 mg mL^{-1}, whereas concentrations of 5.00, 7.50, and 10.00 mg mL^{-1} were considered for Sb_2S_3, Sb_2Se_3 and Sb_2Te_3. All suspensions were prepared following the procedure described below.

An appropriate weight of the dried exfoliated material was suspended in deoxygenated ultrapure water and sonicated for 30 min at a temperature lower than 20 °C. The obtained suspensions were stored in the freezer and were viable for at least one month.

Prior to electrode modification, the modifier suspensions were defrosted and sonicated for 10 min. Then, 5 μL of the modifier suspension was drop-casted onto the working electrode surface ($Ø$ = 4 mm) of a commercial screen-printed carbon electrode (SPCE, DRP-110) purchased from Metrohm DropSens (Oviedo, Spain), and placed in the oven at 25 °C for 30 min for its complete dryness.

2.2.5. Voltammetric measurements

Pb(II) and Cd(II) measurements were developed by differential pulse anodic stripping voltammetry (DPASV). Measurements were carried out using a μAutolab potentiostat System type III purchased from Ecochemie (Utrecht, Netherlands) and attached to a 663 VA Metrohm Stand (Herisau, Switzerland) and a personal computer with GPES software 4.9 version (Ecochemie) to control the system. GPES software was also used for data acquisition and visualization.

Electrochemical experiments were performed in a glass cell with a three-electrode arrangement: Ag/AgCl/KCl (3 mol L^{-1}) as reference electrode, a Pt wire as counter electrode, and the bare SPCE or modified SPCE as working electrode. The working electrode of the SPCE was connected to the potentiostat by means of a flexible cable (ref. CAC) acquired from Metrohm Dropsens. All experiments were carried out without deaeration and at room temperature (20 °C), and all potentials obtained are referred to the Ag/AgCl/KCl (3 mol L^{-1}) electrode.

DPASV measurements were performed in hydrochloric acid 0.01 mol L^{-1} (pH= 2) by applying a deposition potential (E_d) of −1.4 V during a deposition time (t_d) of 240 s with constant stirring, unless otherwise stated. Voltammograms were obtained after 5 s of rest time by scanning the potential from −1.4 to −0.5 V with a modulation time of 50 ms, step potential of 8 mV and a modulation amplitude of 50 mV. A cleaning step (−0.5 V for 30 s under stirring) was applied between measurements.

Before starting the measurements, repeated buffer solution scans were conducted until a constant background signal was obtained. A new modified sensor was used for each experiment, which may include at least 20 measurements.

Calibration curves were recorded by DPASV at the above-established conditions by increasing Cd(II) and Pb(II) concentrations from 0.15 μg mL^{-1} to about 130 μg L^{-1} in 0.01 mol L^{-1} hydrochloric acid (pH= 2) using a bare SPCE, 2D Sb-SPCE, Sb_2S_3-SPCE and Sb_2Se_3-SPCE; and from 25 μg L^{-1} to about 160 μg L^{-1} for Sb_2Te_3-SPCE.

Analysis of the spiked tap water sample was conducted in triplicate using the 2D Sb-SPCE, as the sensor with the best analytical performance, and applying the above-mentioned conditions for DPASV. The water sample was diluted 5-fold and analyzed without any further

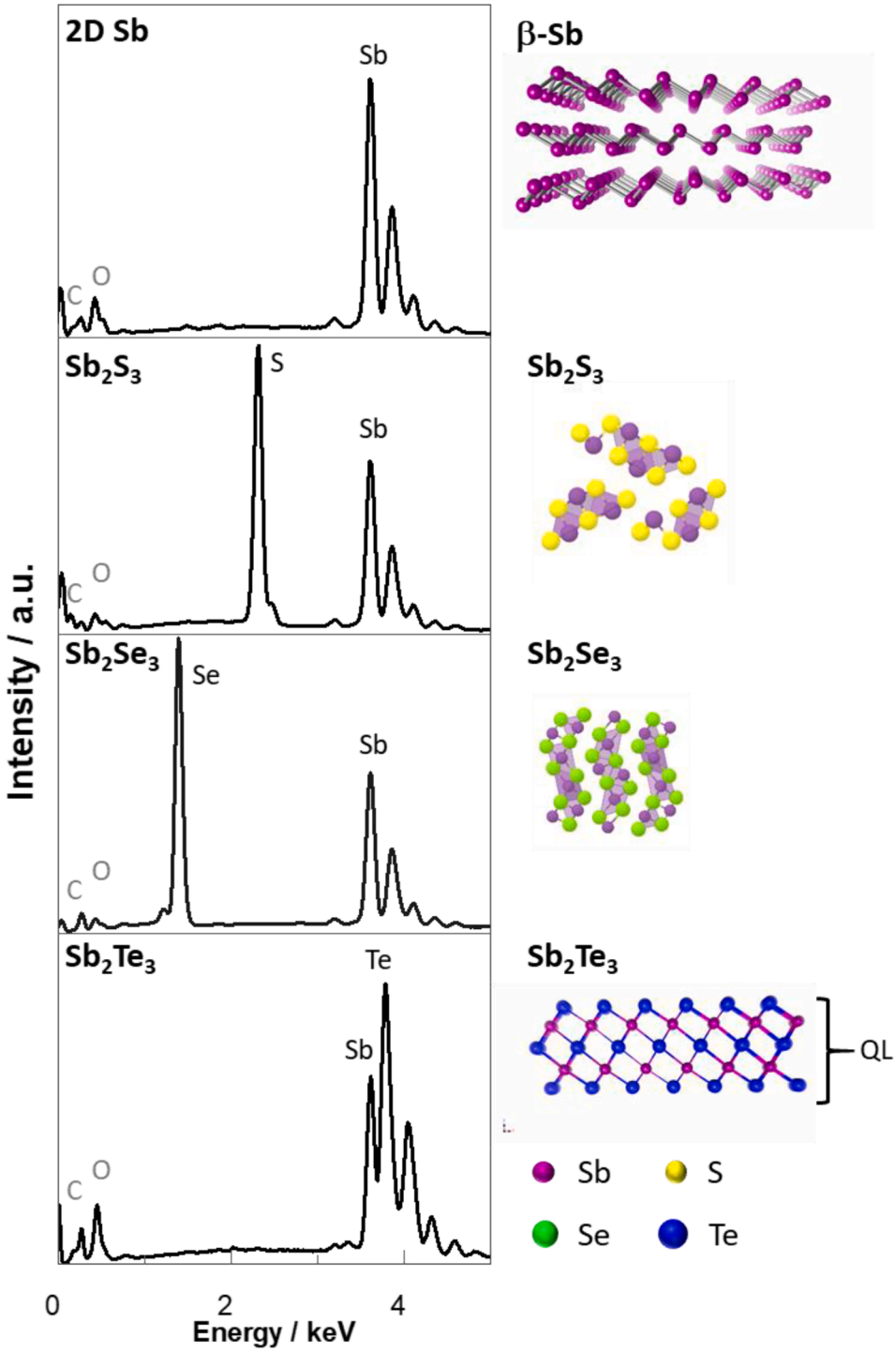

Fig. 1. Crystal structures of 2D Sb, Sb_2S_3, Sb_2Se_3, Sb_2Te_3 and respective EDXS spectra of the materials. The crystal structure of Sb_2Te_3 compromises individual 5 atom thick sheets, quintuple layer (QL in order: Te-Sb-Te-Sb-Te).

pretreatment. The standard addition method was used for calibration by adding three aliquots of Cd(II) and Pb(II) stock solutions and recording the corresponding DP stripping voltammograms.

Inductively coupled plasma mass spectrometry Perkin-Elmer model NexIon 350 D with a collision cell (helium) (USA) was employed for ICP-MS measurements.

3. Results and discussion

3.1. Morphological and chemical characterization

The early elements Sb_2S_3 and Sb_2Se_3 are isomorphous, crystallizing in orthorhombic crystal structure, with 1D nanostructures consisting of immeasurable zigzag ribbons $(Sb_4X_6)_n$ orthorhombic *Pmn* space group, which are held together by weak van der Waals forces and thus enable

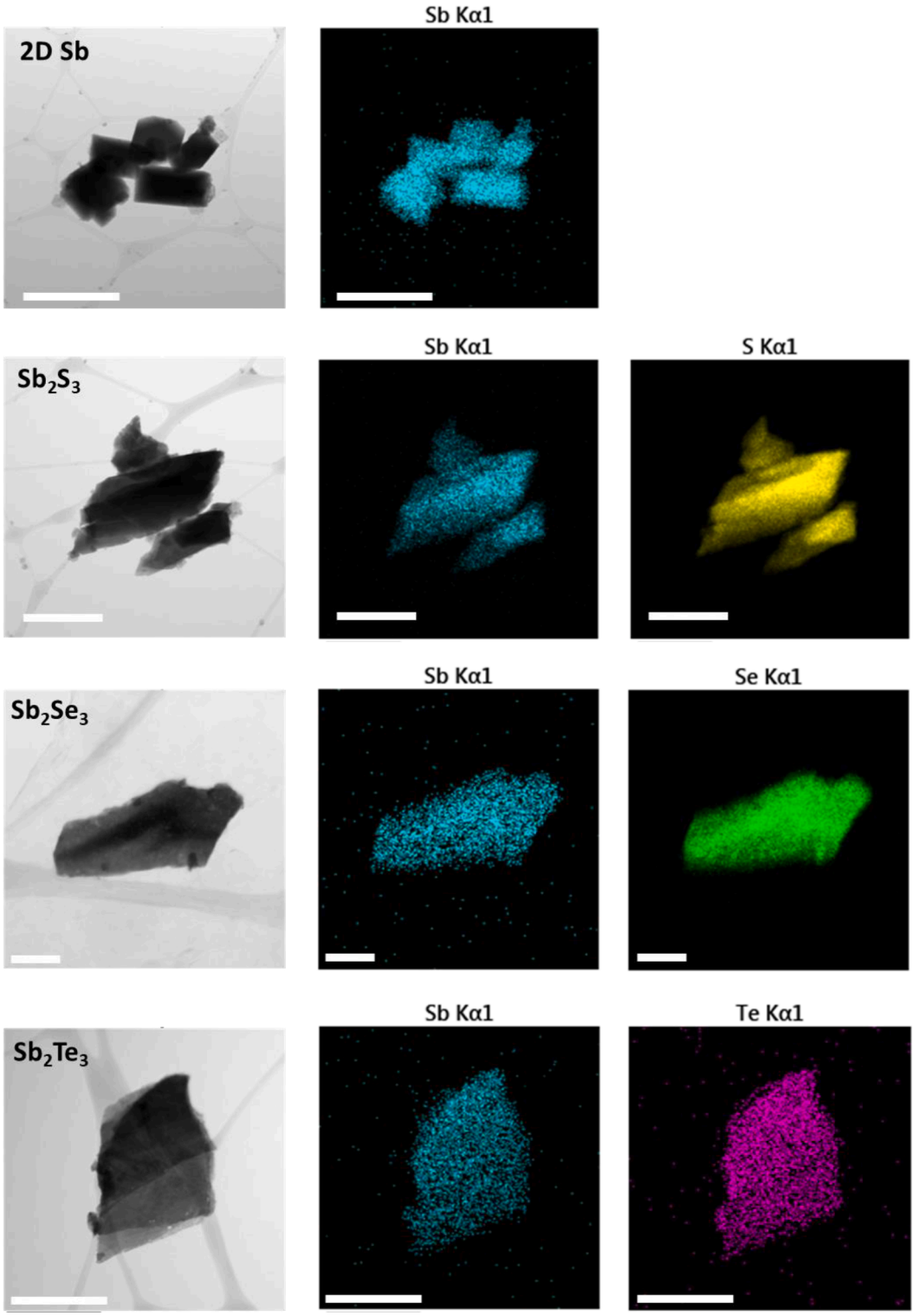

Fig. 2. TEM images of exfoliated 2D Sb, Sb_2S_3, Sb_2Se_3, Sb_2Te_3 and respective EDXS mapping of elements. Scale bars represent 1 μm.

for cleavable along the β-axis direction. In contrast, the hexagonal Sb_2Te_3 and 2D layered monoelement β-Sb (antimonene) are 2D layered materials of rhombohedral structure and $R\bar{3}m$ space group. The crystal structure of the different materials is shown in Fig. 1.

The bulk crystals were analyzed by SEM combined with EDXS. The EDXS spectra of the 2D layered β-Sb (2D Sb) shown in Fig. 1 have the expected peaks profile for antimony at 3.6 keV. For layered Sb_2X_3, additional peaks of the corresponding chalcogenide element are present for S at 2.3 keV, Se at 1.4 keV and Te major peak at 3.8 keV. The latter is overlapped with the peaks assigned to Sb. From each EDXS spectra profiles of the layered Sb_2X_3, the expected Sb/X at.% ratios reached 0.7.

The bulk crystals were subjected to liquid-phase exfoliation by shear force high-speed mixing in aqueous media for 90 min. Fig. 2 shows the morphologies of the exfoliated materials surveyed by TEM images and EDXS. The flakes of 2D Sb have a darker shade, suggesting a thicker material, which can be expected as this material is not constituted by true van der Waals bonded layers. Interlayer interactions are stronger and thus, downsizing is favored instead of delamination.

The EDXS maps of elements shown in Fig. 2 for the processed flakes indicate that 2D Sb and Sb_2X_3 preserve a uniform distribution of the anticipated elements originated from their corresponding starting materials, with noticeable and intense colors for Sb only for 2D Sb, alongside with the more intense corresponding chalcogen element for Sb_2X_3 (X = S, Se, Te) due to their relatively higher content in the exfoliated samples. The high-resolution TEM images of the 2D materials were further analyzed, with the SAED pattern showing that the materials retain good crystallinity (Fig. S1). The average D-spacing between parallel planes calculated was of 0.32 nm for 2D Sb and 0.71 nm for Sb_2Te_3.

3.2. Optimized modification of SPCE with exfoliated materials

Firstly, the experimental conditions for the stripping voltammetric determination of Cd(II) and Pb(II) were optimized using 2D Sb-SPCE.

Acetate buffer 0.1 mol L^{-1} (pH= 4.5) and 0.01 mol L^{-1} hydrochloric acid (pH= 2), as two of the most frequently used supporting electrolytes in the literature, were assessed for the determination of Pb(II) and Cd(II) using 2D Sb-SPCE. Hydrochloric acid 0.01 mol L^{-1} (pH= 2) was chosen as the optimal medium since the peaks obtained for Cd(II) and Pb(II) were better defined as compared to those achieved in acetate buffer (pH= 4.5), especially at lower concentrations.

E_d and t_d were evaluated considering ranges from −0.9 V to −1.4 V and from 30 s to 240 s, respectively. Optimization was carried out in a solution containing 50 μg L^{-1} Pb(II) and Cd(II) at pH= 2.0 (hydrochloric acid) and using a 2D Sb-SPCE prepared from a modifier solution concentration of 1.12 mg mL^{-1}. The compromise selected conditions were an E_d of −1.4 V applied with stirring for 240 s.

With the stripping voltammetric conditions established, different concentrations of modifiers were drop-casted onto the working electrode of the SPCE: from 0.75 to 5.00 mg mL^{-1} for 2D Sb, and from 5.00 to 10.00 mg mL^{-1} for Sb_2S_3, Sb_2Se_3 and Sb_2Te_3.

Fig. 3A-D shows the voltammograms obtained for 20 μg L^{-1} of Pb(II) and Cd(II) using different modifier concentrations of 2D Sb-SPCE (A);

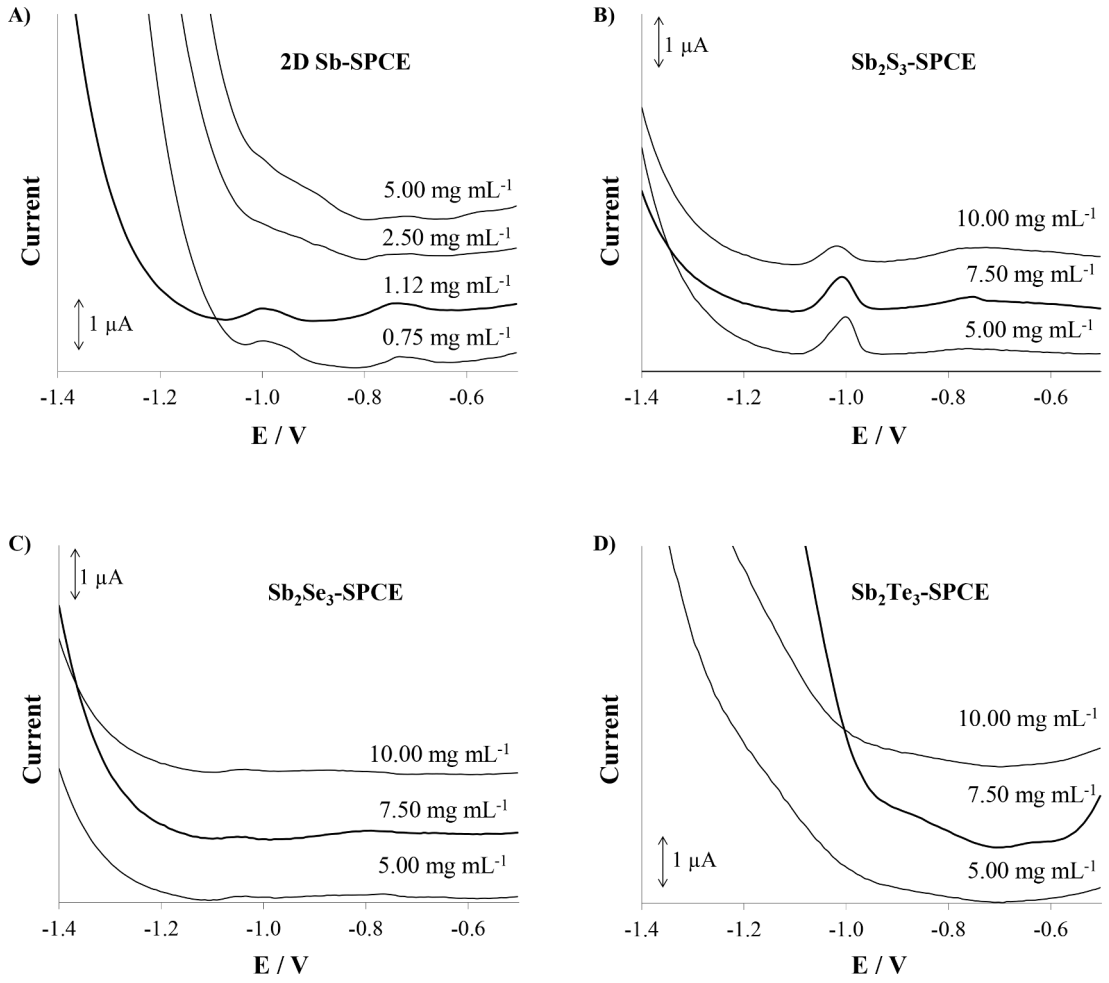

Fig. 3. Effect of the amount of modifiers drop-casted onto the working electrode surface of SPCE on the DP stripping voltammograms for 20 μg L^{-1} of Pb(II) and Cd (II). Electrochemical analysis were performed at pH 2 applying an E_d of −1.4 V during 120 s for 2D Sb-SPCE (A), and 240 s for Sb_2S_3-SPCE (B), Sb_2Se_3-SPCE (C) and Sb_2Te_3-SPCE (D).

Sb_2S_3-SPCE (B), Sb_2Se_3-SPCE (C) and Sb_2Te_3-SPCE (D). In the case of 2D Sb-SPCE the optimal concentration of 2D Sb suspension was 1.12 mg mL^{-1}, whereas for Sb_2S_3, Sb_2Se_3 and Sb_2Te_3 a higher amount of modifier suspensions (7.5 mg mL^{-1}) was required.

3.3. Analytical performance assessment

Once both the SPCE modification and the voltammetric experimental conditions were optimized, calibration curves at increasing concentrations of Pb(II) and Cd(II) from 0.15 μg mL^{-1} to about 130 μg L^{-1} were carried out using 2D Sb-SPCE. Fig. 4A shows representative DP stripping voltammograms obtained using 2D Sb-SPCE with the corresponding calibration plot Fig. 4B. As it can be seen, the calibration curve showed higher voltammetric response as Pb(II) and Cd(II) concentration increased, with well-defined and separated peaks throughout the entire concentration range tested. As it might be expected, 2D Sb-SPCE gave rise to more intense peaks than bare SPCE (Fig. 4C). This can be attributed to the enhanced surface area of the SPCE modified with 2D Sb as well as to the ability of antimonene to accumulate reduced metal ions, both of which enable a more extensive pre-concentration and, therefore,

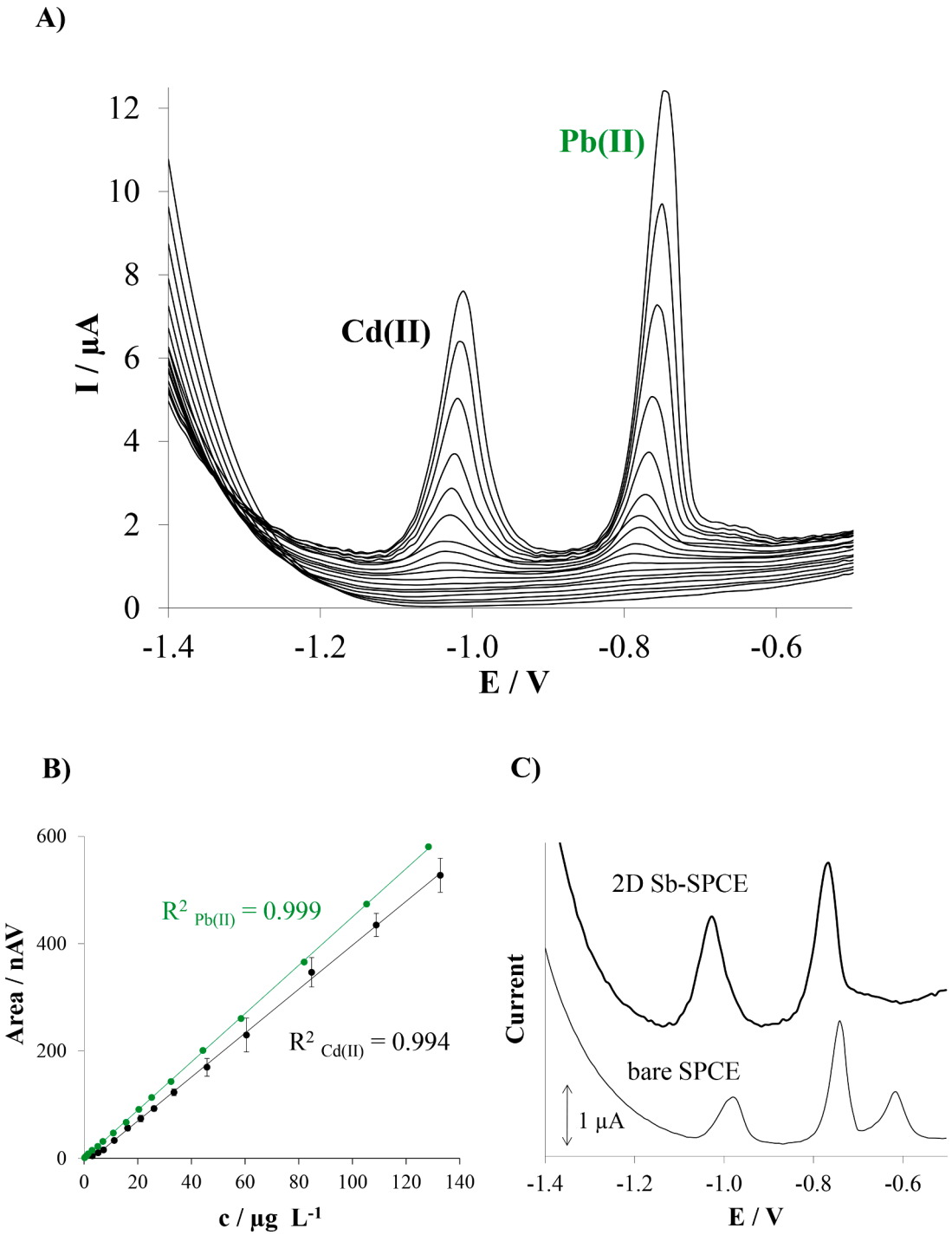

Fig. 4. (A) DP stripping voltammograms and (B) Calibration plots for simultaneous measurements of increasing concentrations of Cd(II) and Pb(II) using 2D Sb-SPCE at pH 2 applying an E_d of −1.4 V during 240 s. C) DPASV measurements of 40 μg L^{-1} Cd(II) and Pb(II) on 2D Sb-SPCE (thick line) and bare SPCE (thin line), at the above-mentioned conditions.

a more quantitative redissolution.

Fig. 5 compares the stripping voltammetric response of 40 μg L^{-1} of Pb(II) and Cd(II) achieved by 2D Sb-SPCE with those obtained by Sb_2S_3-SPCE, Sb_2Se_3-SPCE, Sb_2Te_3-SPCE and bare SPCE. As observed in Fig. 5, the highest voltammetric response for Pb(II) and Cd(II) was recorded using 2D Sb-SPCE, which clearly enhances the DPASV responses achieved not only by bare SPCE but also for the other studied 1D and 2D layered antimony chalcogenides based- sensors. With respect to the latter, the voltammetric response for Cd(II) obtained using Sb_2S_3-SPCE is lower than that achieved by 2D Sb-SPCE but considerably improves the voltammetric response provided by bare SPCE, whereas the Pb(II) and Cd(II) peaks obtained with Sb_2Se_3-SPCE and Sb_2Te_3-SPCE are much lower than those provided by both bare SPCE and 2D Sb-SPCE. These results lead us to assume that antimony chalcogenides have a higher degree of oxidation, thus partially or totally blocking the SPCE surface and hindering an effective accumulation of the target metals ions and, consequently, their reoxidation.

Full calibration curves achieved by bare SPCE, Sb_2S_3-SPCE, Sb_2Se_3-SPCE and Sb_2Te_3-SPCE are also provided in supplementary information (Fig. S2A–D, respectively). Although all calibration curves showed an increased voltammetric response to Pb(II) and Cd(II) with quite well-shaped and resolved peaks, it is again confirmed that the 2D Sb-SPCE is the one that gives rise to both higher voltammetric stripping peaks and flatter voltammetric stripping baseline.

The analytical performance of 2D Sb-SPCE was compared with those provided by bare SPCE and layered antimony chalcogenides based-sensors. The parameters evaluated for the analytical performance assessment are summarized in Table 1, considering for comparison the sensitivity as the slope of the calibration plot, the linear range with its respective coefficient of determination (R^2) and the limit of detection (LOD), which was calculated as 3 times the standard deviation of the intercept over the slope of the calibration plot. The lower value of the linear range was stated as the limit of quantification (LOQ), which was designed as 10 times the precedent ratio.

Comparing all the tested electrodes, the one with the best analytical performance was the 2D Sb-SPCE. As observed in Table 1 the 2D Sb-SPCE provides high sensitivities, linear ranges until 128.3 and 132.7 μg L^{-1} for Pb(II) and Cd(II) respectively with R^2 very close to 1, and LOD values of 0.3 and 2.7 μg L^{-1} for Pb(II) and Cd(II), respectively. These obtained results lead us to conclude that the modification with 2D Sb can perfectly be adapted to SPCE and be further applied to the analyses of Pb (II) and Cd(II) in water samples at concentrations below the maximum contaminant level set by the World Health Organization for drinking water [21]. In contrast, it should be noticed that layered antimony chalcogenides based- sensors, and particularly Sb_2Se_3-SPCE and Sb_2Te_3-SPCE, give rives to much narrower linear ranges with low correlation, which makes them not fully recommendable for the anodic stripping voltammetric determination of studied metal ions, contrasting with their proven success in other electrochemical fields such as energy conversion and storage [15].

Repeatability and reproducibility were tested for 2D Sb-SPCE as the best of the assessed electrodes and were compared to those obtained by bare SPCE. Repeatability was expressed as the relative standard deviation (RSD,%) of five consecutive measurements of 25 μg L^{-1} of Pb(II) and Cd(II) using the same electrode, whereas reproducibility was stated as the RSD (%) for three different 2D Sb-SPCE within series of five

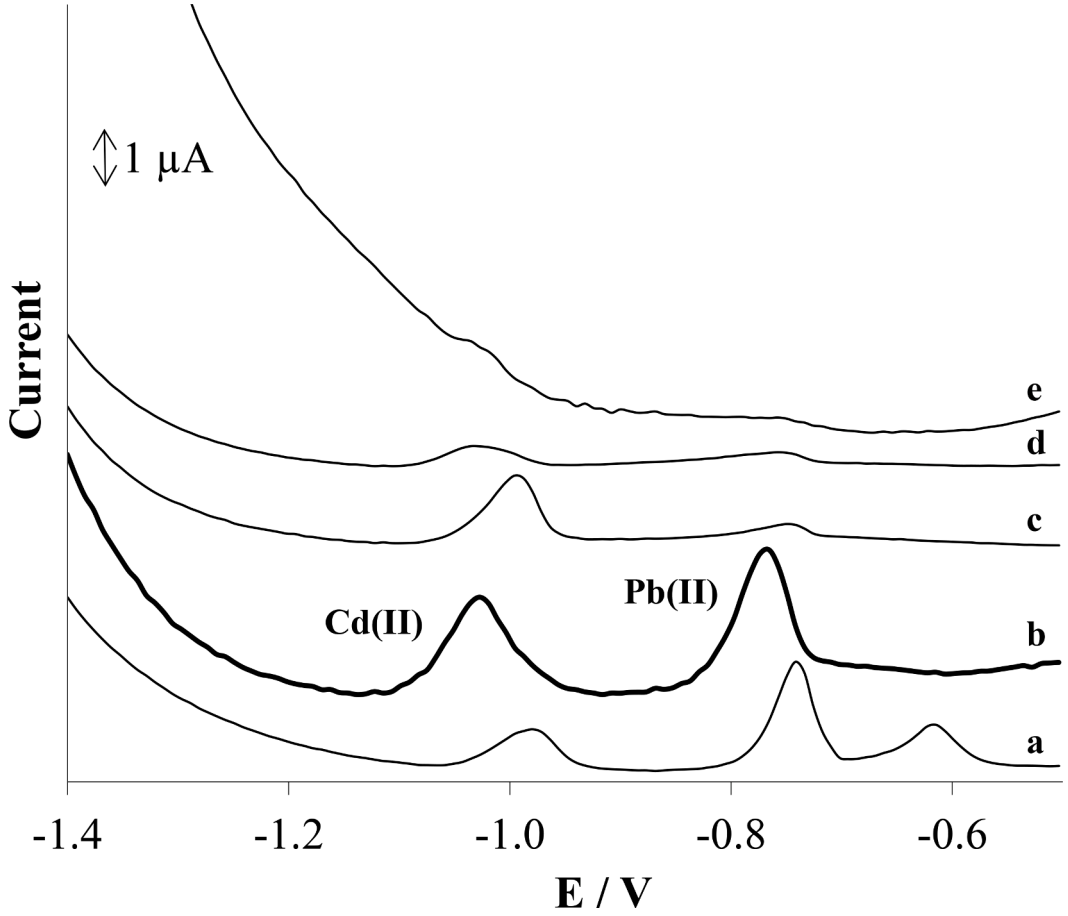

Fig. 5. Comparative DP stripping voltammograms for 40 μg L^{-1} of Cd(II) and Pb(II) recorded for the tested electrodes at the optimal amount of modifier: (a) bare SPCE, (b) 2D Sb-SPCE, (c) Sb_2S_3-SPCE, (d) Sb_2Se_3-SPCE, and (e) Sb_2Te_3-SPCE. Electrochemical analysis were performed at pH 2 applying an E_d of −1.4 V during 240 s.

Table 1
Analytical performance for the DPASV simultaneous determination of Pb(II) and Cd(II) using bare SPCE, 2D Sb-SPCE, Sb_2S_3-SPCE, Sb_2Se_3-SPCE, Sb_2Te_3-SPCE at pH 2, E_d −1.4 V and t_d 240 s. The standard deviations are shown within brackets.

	bare SPCE		2D Sb-SPCE		Sb_2S_3-SPCE		Sb_2Se_3-SPCE		Sb_2Te_3-SPCE	
	Pb(II)	Cd(II)	Pb(II)	Cd(II)	Pb(II)	Cd(II)	Pb(II)	Cd(II)	Pb(II)	Cd(II)
Sensitivity (nA V μg^{-1} L)	6.1(0.2)	2.9(0.1)	4.50(0.01)	4.09(0.06)	0.49(0.01)	1.90(0.07)	0.63(0.02)	0.47(0.05)	0.95(0.05)	1.1(0.1)
Intercept (μg L^{-1})	−140(10)	−61(6)	−0.5(0.5)	−12(4)	−0.3(0.3)	−17(3)	−0.4(0.6)	−3.0(0.7)	−47(5)	−60(10)
Linear range (μg L^{-1})[a]	18.0–101.0	20.2–104.5	1.1–128.3	9.1–132.7	6.0–49.4	15.4–104.0	9.8–49.4	14.5–18.5	57.5–157.3	89.5–161.5
R^2	0.989	0.987	0.999	0.994	0.986	0.969	0.976	0.915	0.958	0.907
LOD (μg L^{-1})	5.4	6.1	0.3	2.7	1.8	4.6	3.0	4.3	17.3	26.9

[a] The lowest level of the linear range was established from the LOQ.

consecutive measurements. The proposed 2D Sb-SPCE owns a remarkable repeatability (1.7% and 0.7% for Pb(II) and Cd(II), respectively) and a good reproducibility (4.8% and 1.0% for Pb(II) and Cd(II), respectively) as compared to those achieved by bare SPCE (repeatability of 4.2% and 9.3%, and reproducibility of 9.2% and 9.6% for Pb(II) and Cd(II), respectively).

Regarding previous results, it should be pointed out that the direct comparison with other electrodes based on 2DSb or 1D, 2D layered antimony chalcogenides is not possible because the use of these materials has not been reported for the voltammetric determination of metal ions yet. Nevertheless, as compared to electrodes based on other forms of antimony (Table 2), the results obtained using 2D Sb-SPCE show significant improvements on the LOD values achieved by 2D Sb-SPCE, especially for Pb(II), since its LOD is much lower than most of those reported in previous studies using other antimony-based electrodes. In the case of Cd(II), a comparable LOD value was achieved. Regarding linear ranges, wider working ranges are available as compared to the linear ranges up to or below 100 μg L^{-1} stated in most of the published studies.

Another important consideration is the modification procedure required for the development of the sensor. In particular, the 2D Sb-SPCE involves an easy and very fast procedure based on the drop-casting of few μL of the 2D Sb suspension on the SPCE surface that can be used as purchased without further polishing procedures or pretreatments. However, most of the reported sensors comprise more complex and time-consuming modification processes either for the formation of the Sb film or for the pretreatments required when the sensor was developed in a non-disposable platform.

Table 2
Analytical performance of antimony based electrodes developed since 2010 for the simultaneous stripping voltammetric determination of Cd(II) and Pb(II).

Electrode	Technique	Linear range (μg L^{-1})		LOD (μg L^{-1})		Deposition time (s)	Refs.
		Cd(II)	Pb(II)	Cd(II)	Pb(II)		
In-situ Sb-GCE	SWASV	5.2–110	4.7–120	1.7	1.5	120	[22]
Ex-situ porous Sb-AuE	DPASV	20–120	20–120	0.7	0.5	100	[23]
Ex-situ Sb-AuE	DPASV	20–120	20–120	2.8	1.8	100	
In-situ Sb-CFME	DPASV	20–100	20–100	1.9	3.1	120	[24]
Bulk Sb-CPE	SWASV	20–120	20–120	1.4	0.9	300	[25]
Bulk Sb-CPE	SCP	10–100	10–100	1.5	2.8	300	
Sb_2O_3–CPE	SWASV	10–100	10–100	1	0.7	90	[26]
Sb_2O_3–CPE	SCP	10–100	10–100	1	1	90	
In-situ Sb-SPCE	DPASV	10–90	5–45	2.7	1.0	240	[27]
Bulk Sb_2O_3-SPCE	DPASV	10–90	5–45	2.5	0.9	240	
Bulk $Sb(C_2O_4)OH$-SPCE	DPASV	10–90	5–45	3.5	1.1	240	
Bulk ATO-SPCE	DPASV	10–90	5–45	1.8	1.1	240	
In-situ Sb/Bi-CPE	SWASV	10–70	10–70	0.8	0.9	300	[28]
Ex-situ Sb/Bi-CPE	SWASV	10–70	10–70	1.1	1.4	300	
Ex-situ Sb/Nafion-GCE	DPAdSV	0.9–12.0	0.9–12.0	0.4	0.5	100	[29]
In-situ Sb/Nafion-GCE	SWASV	10–150	10–150	0.05	0.05	120	[30]
In-situ Sb-GCE	SWASV	10–150	10–150	0.5	0.5	120	
Bulk SbNP-MWCNT-CPE	SWASV	10–60	10–60	0.77	0.65	120	[31]
Ex-situ Sb-GCE	DPASV	n.s.	n.s.	2.32	2.65	300	[32]
In-situ Sb-SPCE	DPASV	11.5–72.4	16.8–62.6	3.4	5.0	120	[33]
Ex-situ PEDOT-SDS-Sb-GCE	SWASV	4.5–140.0	4.5–140.0	0.80	0.50	60	[34]
Ex-situ Sb-SPAN/EG	DPASV	2–70	2–70	0.41	0.20	180	[35]
In-situ Sb-SPCE	DPASV	9.5–100.3	17.5–100.9	2.8	5.3	120	[36]
In-situ Sb-SPGPHE	DPASV	13.2–100.3	28.8–100.9	4.0	8.6	120	
In-situ Sb-SPMWCNTE	DPASV	8.6–100.3	14.7–100.9	2.6	4.4	120	
In-situ Sb-SPCNFE	DPASV	3.7–100.3	6.9–100.9	1.1	2.1	120	
In-situ Sb-GO-SPCE	SI-SWASV	33.7–168.6	20.7–269.36	6.07	5.39	100	[37]
In-situ Sb-MCM41/Nafion/GCE	SWASV	5–30	5–30	0.29	0.08	400	[38]
In-situ Sb-GCE	SWASV	5.0–224	14.8–267.7	3.0	6.0	60	[39]
In-situ Sb-IMCE	SWASV	0–120	0–120	1.3	0.95	240	[40]
rGO/SbNP-GCE	SWASV	11.2–337.2	20.7–621.6	7.8	9.4	150	[41]
Bulk Sb_2O_3–MWCNT-CPE	LSASV	80–150	5–35	16.77	6.12	600	[42]
2D Sb-SPCE	DPASV	9.1–132.7	1.1–128.3	2.7	0.3	240	This work

ATO: antimony tin oxide; AuE: gold electrode; CFME: carbon fiber microelectrode; CPE: carbon paste electrode; DPAdSV: differential pulse adsorptive stripping voltammetry; DPASV: differential pulse anodic stripping voltammetry; GCE: glassy carbon electrode; GO: graphene oxide; IMCE: injection molded conductive electrode; MWCNTs: multiwall carbon nanotubes; n.s. not specified; PEDOT-SDS: poly(3,4-ethylenedioxythiophene)-sodium dodecyl sulfate; rGO: reduced graphene oxide; SbNP: antimony nanoparticles; SCP: stripping chronopotentiometry; SI: sequential injection; SPAN-EG: self-doped sulfonated polyaniline/expanded graphite; SPCE: screen-printed carbon electrode; SPCNFE: screen-printed carbon nanofiber electrode; SPGPHE: screen-printed graphene electrode; SPMWCNTE: screen-printed multiwalled carbon nanotubes electrode; SWASV: square wave anodic stripping voltammetry.

Contrasting the performance of the 2D Sb-SPCE with that achieved by bismuthene carbon-based screen-printed electrode (2D Bi-SPCE) [12], it can be stated that the 2D Bi-SPCE provided lower LODs (0.06 and 0.07 μg L^{-1} for Pb(II) and Cd(II) respectively), but narrower linear ranges (up to 25 μg L^{-1} for Pb(II) and Cd(II)) and lower sensitivities (2.76 and 2.32 nA V $μg^{-1}$ L for Pb(II) and Cd(II), respectively) for both metal ions. Moreover, it should be taken into account that 2D Sb-SPCE allows working at more acidic pH and that the potential window available for the voltammetric determination of metal ions using a 2D Sb-SPCE is much wider than that offered by 2D Bi-SPCE since the Sb oxidation peak appears at more positive potentials than Bi oxidation peak.

3.4. Application to the analysis of a real sample

The suitability of 2D Sb-SPCE for the simultaneous determination of Pb(II) and Cd(II) was verified by the DPASV analysis of a spiked tap water sample. The tap water sample was fortified with 160.5 μg L^{-1} of Pb(II) and 111.7 μg L^{-1} of Cd(II) and diluted 5-fold for the voltammetric determination without further treatment. DPASV measurements of the spiked water sample together with three additions of Pb(II) and Cd(II) were carried out in triplicate at the above-mentioned conditions. The standard addition method was used for the determination of target metal ions. Fig. 6A displays characteristic DPAS voltammograms achieved in the determination of the tap water sample using 2D Sb-SPCE. Well-shaped and separated peaks for both considered metal ions were achieved. The standard addition plot (Fig. 6B) illustrates for both Pb(II) and Cd(II) the good correlation between the measurements performed using 2D Sb-SPCE.

The results of the Pb(II) and Cd(II) concentration computed from three replicates of the spiked tap water sample by DPASV carried out using 2D Sb-SPCE are summarized in Table 3. The obtained results presented a good precision as can be inferred from the low RSD (%) values obtained. In order to assess the accuracy of the presented method

Table 3
Total concentrations of Pb(II) and Cd(II) determined in spiked tap water sample by DPASV using 2D Sb-SPCE and by ICP-MS. DPASV measurements were carried out by the standard addition method at pH 2 applying a deposition potential of −1.4 V during 240 s.

		Pb(II)	Cd(II)
DPASV	C (μg L^{-1})	157.3	111.6
	RSD (%)	4.2	3.0
ICP-MS	C (μg L^{-1})	163.2	117.6
	RSD (%)	0.9	0.6

$n = 3$ was considered for RSD (%).

the spiked tap water sample was also analysed by ICP-MS (Table 3), and the results attained from both DPASV using 2D Sb-SPCE and ICP-MS were statistically evaluated. For this purpose, a two-tailed *t*-test (non-equal variances) was carried and it was determined that the DPASV using 2D Sb-SPCE and ICP-MS provided statistically comparable results for a confidence level of 95% (t-statistic for Pb(II)= 1.53; t-statistic for Cd(II)= 3.07; and critical value of t (two-tailed)= 4.30). Therefore, it can be concluded that the obtained DPASV results presented good accuracy. Moreover, the DPASV method coupled with 2D Sb-SPCE can be considered as a suitable alternative to the most conventional ICP-MS method for the simultaneous determinations of Pb(II) and Cd(II) in real samples. Furthermore, the possibility to attach SPEs to portable instrumentation represents a great advantage for the on-site determination or monitoring of the target metal ions with a lower cost and allowing a more agile and immediate response in case of a contamination scenario.

4. Conclusions

To sum up, this work reports the development of 2D Sb-based modified screen-printed electrode prepared by drop-casting of an

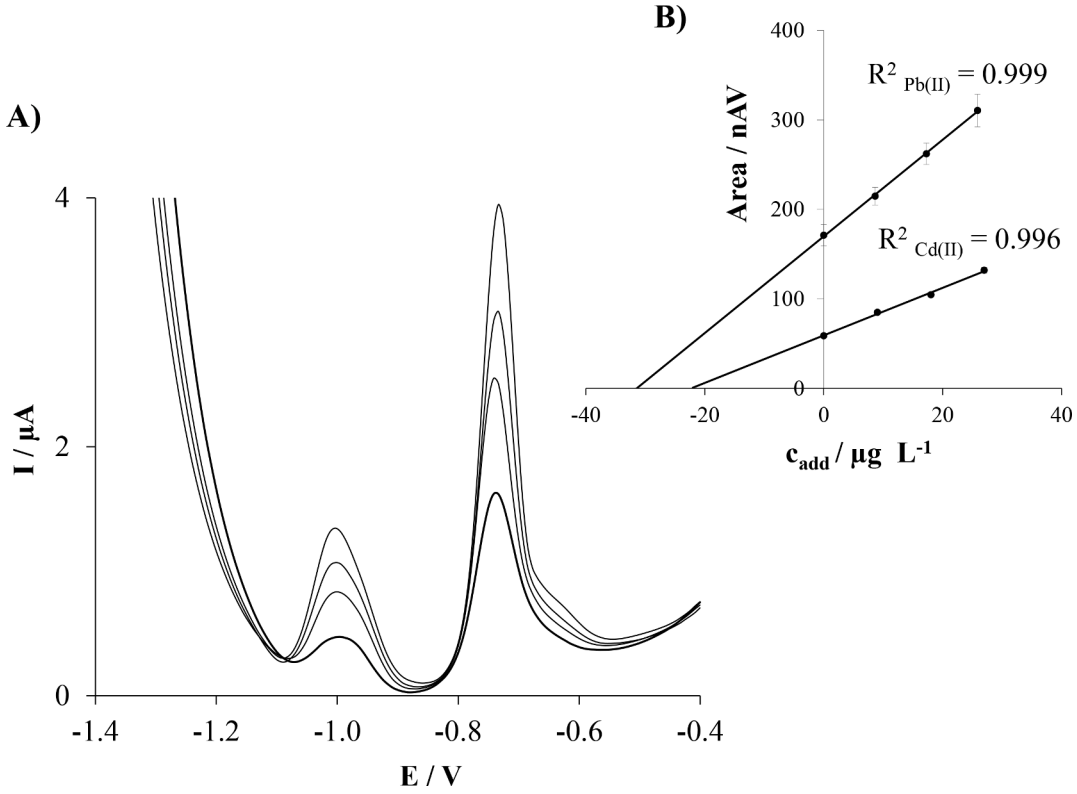

Fig. 6. (A) Representative DP stripping voltammograms in a spiked tap water sample using a 2D Sb-SPCE at pH 2 applying an E_d of −1.4 V during 240 s; (B) Standard addition plots.

exfoliated layered antimony suspension onto the working electrode. Similarly, SPCEs were also modified with the corresponding antimony chalcogenides (1D Sb_2S_3, 1D Sb_2Se_3 and 2D Sb_2Te_3). The materials were delaminated by liquid-phase exfoliation and characterized by TEM/EDXS.

The analytical performance of 2D Sb-SPCE was contrasted to those achieved by both bare SPCE and layered antimony chalcogenides based-SPCEs, concluding that 2D Sb-SPCE displays enhanced electrochemical and analytical features in comparison with the bare SPCE and is a much more appropriate choice than the corresponding 1D and 2D layered antimony chalcogenides for the determination of Pb(II) and Cd(II) by DPASV. The reached LODs and linear ranges were not only better than those attained by bare SPCE and layered antimony chalcogenides based-sensors but also comparable or even much improved than values stated in earlier works for antimony- based electrodes with other supports or modification methods. It should also be noticed that, as compared to bismuthene- modified screen-printed electrode, wider linear ranges and higher sensitivities for both metal ions were obtained with 2D Sb-SPCE, without forgetting that the work at more acidic pH with a wider potential window is feasible. In addition, the reproducibility and repeatability of 2D Sb-SPCE are excellent as compared to the bare SPCE. Thus, the excellent analytical performance of 2D Sb as modifier together with the benefits of using SPEs as disposable and low-cost platforms, endorse their use for the determination of very low concentrations of metal ions in water samples.

The practical applicability of the DPASV method using 2D Sb-SPCE for the determination of Pb(II) and Cd(II) in spiked tap water samples was demonstrated by obtaining statistically comparable results to those attained by ICP-MS measurements.

CRediT authorship contribution statement

María A. Tapia: Methodology, Formal analysis, Investigation, Visualization. **Clara Pérez-Ràfols:** Methodology, Formal analysis, Writing – original draft, Visualization, Resources. **Jan Paštika:** Formal analysis, Investigation, Visualization. **Rui Gusmão:** Conceptualization, Methodology, Formal analysis, Writing – original draft, Visualization, Supervision, Resources. **Núria Serrano:** Conceptualization, Methodology, Formal analysis, Writing – original draft, Visualization, Supervision, Resources. **Zdeněk Sofer:** Methodology, Writing – review & editing, Visualization, Resources. **José Manuel Díaz-Cruz:** Methodology, Formal analysis, Validation, Writing – review & editing, Visualization, Resources.

Declaration of Competing Interest

The authors declare that they have no known competing financial interests or personal relationships that could have appeared to influence the work reported in this paper.

Acknowledgments

This work was financially supported by the Ministry of Science and Innovation of Spain (Project PID2019–107102RB-C22). The support (without funding) of the Generalitat of Catalonia (Project 2017SGR-311) is also acknowledged. M.A.T. gratefully acknowledge the Peruvian National Programme of Scholarships and Student loans (PRONABEC) for her Ph.D grant (Beca president de la República-343245), and the support of the Water Research Institute (IdRA) of the University of Barcelona. Financial support from the Czech Science Foundation (Project GACR No 19–26910X) is also gratefully acknowledged.

Supplementary materials

Supplementary material associated with this article can be found, in the online version, at doi:10.1016/j.electacta.2022.140690.

References

[1] J. Barton, M.B.G. García, D.H. Santos, P. Fanjul-Bolado, A. Ribotti, M. McCaul, D. Diamond, P. Magni, Screen-printed electrodes for environmental monitoring of heavy metal ions: a review, Microchim. Acta 183 (2016) 503–517, https://doi.org/10.1007/s00604-015-1651-0.
[2] C. Ariño, N. Serrano, J.M. Díaz-Cruz, M. Esteban, Voltammetric determination of metal ions beyond mercury electrodes. A review, Anal. Chim. Acta 990 (2017) 11–53, https://doi.org/10.1016/j.aca.2017.07.069.
[3] J. Wang, Stripping analysis at bismuth electrodes: a review, Electroanalysis 17 (2005) 1341–1346, https://doi.org/10.1002/elan.200403270.
[4] S.B. Hocevar, I. Švancara, B. Ogorevc, K. Vytřas, Antimony film electrode for electrochemical stripping analysis, Anal. Chem. 79 (2007) 8639–8643, https://doi.org/10.1021/ac070478m.
[5] N. Serrano, J.M. Díaz-Cruz, C. Ariño, M. Esteban, Antimony- based electrodes for analytical determinations, TrAC Trends Anal. Chem. 77 (2016) 203–213, https://doi.org/10.1016/j.trac.2016.01.011.
[6] N. Serrano, A. Alberich, J.M. Díaz-Cruz, C. Ariño, M. Esteban, Coating methods, modifiers and applications of bismuth screen-printed electrodes, TrAC Trends Anal. Chem. 46 (2013) 15–29, https://doi.org/10.1016/j.trac.2013.01.012.
[7] M. Chhowalla, D. Jena, H. Zhang, Two-dimensional semiconductors for transistors, Nat. Rev. Mater. 1 (2016) 16052, https://doi.org/10.1038/natrevmats2016.52.
[8] P.K. Kannan, D.J. Late, H. Morgan, C.S. Rout, Recent developments in 2D layered inorganic nanomaterials for sensing, Nanoscale 7 (2015) 13293–13312, https://doi.org/10.1039/c5nr03633j.
[9] F. Tseliou, A. Avgeropoulos, P. Falaras, M.I. Prodromidis, Low dimensional Bi_2Te_3-graphene oxide hybrid film-modified electrodes for ultra-sensitive stripping voltammetric detection of Pb(II) and Cd(II), Electrochim. Acta 231 (2017) 230–237, https://doi.org/10.1016/j.electacta.2017.02.058.
[10] S. Zhang, S. Guo, Z. Chen, Y. Wang, H. Gao, J. Gómez-Herrero, P. Ares, F. Zamora, Z. Zhu, H. Zeng, Recent progress in 2D group-VA semiconductors: from theory to experiment, Chem. Soc. Rev. 47 (2018) 982–1021, https://doi.org/10.1039/c7cs00125h.
[11] M.A. Tapia, R. Gusmão, N. Serrano, Z. Sofer, C. Ariño, J.M. Díaz-Cruz, M. Esteban, Phosphorene and other layered pnictogens as a new source of 2D materials for electrochemical sensors, TrAC Trends Anal. Chem. 139 (2021), 116249, https://doi.org/10.1016/j.trac.2021.116249.
[12] M.A. Tapia, C. Pérez-Ràfols, R. Gusmão, N. Serrano, Z. Sofer, J.M. Díaz-Cruz, Enhanced voltammetric determination of metal ions by using a bismuthene-modified screen-printed electrode, Electrochim. Acta 362 (2020), 137144, https://doi.org/10.1016/j.electacta.2020.137144.
[13] A.Ch. Lazanas, K. Tsirka, A.S. Paipetis, M.I. Prodromidis, 2D bismuthene/graphene modified electrodes for the ultra-sensitive stripping voltammetric determination of lead and cadmium, Electrochim. Acta 336 (2020), 135726, https://doi.org/10.1016/j.electacta.2020.135726.
[14] H. Lei, J. Chen, Z. Tan, G. Fang, Review of recent progress in antimony chalcogenide-based solar cells: materials and devices, Sol. RRL 3 (2019), 1900026, https://doi.org/10.1002/solr.201900026.
[15] R. Gusmão, Z. Sofer, J. Luxa, M. Pumera, Antimony chalcogenide van der waals nanostructures for energy conversion and storage, ACS Sustain. Chem. Eng. 7 (2019) 15790–15798, https://doi.org/10.1021/acssuschemeng.9b04415.
[16] B. Fatima, D. Hussain, S. Bashir, H.T. Hussain, R. Aslam, R. Nawaz, H.N. Rashid, N. Bashir, S. Majeed, M.N. Ashiq, M. Najam-ul-Haq, Catalase immobilized antimonene quantum dots used as an electrochemical biosensor for quantitative determination of H_2O_2 from CA-125 diagnosed ovarian cancer samples, Mater. Sci. Eng. C 117 (2020), 111296, https://doi.org/10.1016/j.msec.2020.111296.
[17] A.Ch. Lazanas, M.I. Prodromidis, Electrochemical performance of passivated antimonene nanosheets and of *in-situ* prepared antimonene oxide-PEDOT:PSS modified screen-printed graphite electrodes, Electrochim. Acta 410 (2022), 140033, https://doi.org/10.1016/j.electacta.2022.140033.
[18] C.C. Mayorga-Martinez, R. Gusmão, Z. Sofer, M. Pumera, Pnictogen-based enzymatic phenol biosensors: phosphorene, arsenene, antimonene, and bismuthene, Angew. Chem. 131 (2019) 140–144, https://doi.org/10.1002/ange.201808846.
[19] T. García-Mendiola, C. Gutiérrez-Sánchez, C. Gibaja, I. Torres, C. Busó-Rogero, F. Pariente, J. Solera, Z. Razavifar, J.J. Palacios, F. Zamora, E. Lorenzo, Functionalization of a few-layer antimonene with oligonucleotides for DNA sensing, ACS Appl. Nano Mater. 3 (2020) 3625–3633, https://doi.org/10.1021/acsanm.0c00335.
[20] M.A. Tapia, R. Gusmão, C. Pérez-Ràfols, X. Subirats, N. Serrano, Z. Sofer, J.M. Díaz-Cruz, Enhanced voltammetric performance of sensors based on oxidized 2D layered black phosphorus, Talanta 238 (2022), 123036, https://doi.org/10.1016/j.talanta.2021.123036.
[21] World Health Organization, Guidelines For Drinking-Water quality: Fourth Edition Incorporating the First Addendum, World Health Organization, Geneva, 2017.
[22] V. Guzsvány, H. Nakajima, N. Soh, K. Nakano, T. Imato, Antimony-film electrode for the determination of trace metals by sequential-injection analysis/anodic stripping voltammetry, Anal. Chim. Acta 658 (2010) 12–17, https://doi.org/10.1016/j.aca.2009.10.049.
[23] V. Urbanová, K. Vytřas, A. Kuhn, Macroporous antimony film electrodes for stripping analysis of trace heavy metals, Electrochem. Commun. 12 (2010) 114–117, https://doi.org/10.1016/j.elecom.2009.11.001.
[24] M. Slavec, S.B. Hocevar, L. Baldrianova, E. Tesarova, I. Svancara, B. Ogorevc, K. Vytras, Antimony film microelectrode for anodic stripping measurement of cadmium(II), lead(II) and copper(II), Electroanalysis 22 (2010) 1617–1622, https://doi.org/10.1002/elan.200900583.

[25] E. Svobodova-Tesarova, L. Baldrianova, M. Stoces, I. Svancara, K. Vytras, S. B. Hocevar, B. Ogorevc, Antimony powder-modified carbon paste electrodes for electrochemical stripping determination of trace heavy metals, Electrochim. Acta 56 (2011) 6673–6677, https://doi.org/10.1016/j.electacta.2011.05.048.
[26] E. Svobodová, L. Baldrianová, S.B. Hočevar, I. Švancara, Electrochemical stripping analysis of selected heavy metals at antimony trioxide-modified carbon paste electrode, Int. J. Electrochem. Sci. 7 (2012) 197–210.
[27] M. Maczuga, A. Economou, A. Bobrowski, M.I. Prodromidis, Novel screen-printed antimony and tin voltammetric sensors for anodic stripping detection of Pb(II) and Cd(II), Electrochim. Acta 114 (2013) 758–765, https://doi.org/10.1016/j.electacta.2013.10.075.
[28] A.M. Ashrafi, K. Vytřas, Codeposited antimony-bismuth film carbon paste electrodes for electrochemical stripping determination of trace heavy metals, Int. J. Electrochem. Sci. 8 (2013) 2095–2103.
[29] V. Arancibia, E. Nagles, C. Rojas, M. Gómez, *Ex situ* prepared nafion-coated antimony film electrode for adsorptive stripping voltammetry of model metal ions in the presence of pyrogallol red, Sens. Actuators B Chem. 182 (2013) 368–373, https://doi.org/10.1016/j.snb.2013.03.014.
[30] Z. Zhang, J. Zheng, Y. Zhang, W. Zhang, L. Li, Z. Cao, H. Wang, C. Li, Y. Gao, J. Liu, Anti-fouling *in situ* deposited antimony/nafion film electrode for electrochemical stripping analysis, Int. J.Electrochem. Sci. 8 (2013) 4183–4193.
[31] A.M. Ashrafi, S. Cerovac, S. Mudrić, V. Guzsvány, L. Husáková, I. Urbanová, K. Vytřas, Antimony nanoparticle-multiwalled carbon nanotubes composite immobilized at carbon paste electrode for determination of trace heavy metals, Sens. Actuators B Chem. 191 (2014) 320–325, https://doi.org/10.1016/j.snb.2013.08.087.
[32] M.K. Dey, A.K. Satpati, A.V.R. Reddy, Electrodeposited antimony and antimony-gold nanocomposite modified carbon paste electrodes for the determination of heavy metal ions, Anal. Methods 6 (2014) 5207–5213, https://doi.org/10.1039/c4ay00876f.
[33] V. Sosa, C. Barceló, N. Serrano, C. Ariño, J.M. Díaz-Cruz, M. Esteban, Antimony film screen-printed carbon electrode for stripping analysis of Cd(II), Pb(II), and Cu (II) in natural samples, Anal. Chim. Acta 855 (2015) 34–40, https://doi.org/10.1016/j.aca.2014.12.011.
[34] E. Nagles, O. García-Beltrán, J. Hurtado, *Ex situ* poly(3,4-ethylenedioxythiophene)-sodium dodecyl sulfate-antimony film electrode for anodic stripping voltammetry determination of lead and cadmium, Int. J. Electrochem. Sci. 11 (2016) 7507–7518, https://doi.org/10.20964/2016.09.28.
[35] R. Liu, H. Cao, Z. Nie, S. Si, X. Zhao, X. Zeng, A disposable expanded graphite paper electrode with self-doped sulfonated polyaniline/antimony for stripping voltammetric determination of trace Cd and Pb, Anal. Methods 8 (2016) 1618–1625, https://doi.org/10.1039/c5ay03094c.
[36] C. Pérez-Ràfols, N. Serrano, J.M. Díaz-Cruz, C. Ariño, M. Esteban, New approaches to antimony film screen-printed electrodes using carbon-based nanomaterials substrates, Anal. Chim. Acta 916 (2016) 17–23, https://doi.org/10.1016/j.aca.2016.03.003.
[37] P. Ruengpirasiri, E. Punrat, O. Chailapakul, S. Chuanuwatanakul, Graphene oxide-modified electrode coated with *in-situ* antimony film for the simultaneous determination of heavy metals by sequential injection-anodic stripping voltammetry, Electroanalysis 29 (2017) 1022–1030, https://doi.org/10.1002/elan.201600568.
[38] Y. Yin, H. Wang, G. Liu, Electrochemical detection of trace cadmium and lead on a MCM41/nafion/antimony film composite-modified electrode, Int. J. Electrochem. Sci. 13 (2018) 10259–10273, https://doi.org/10.20964/2018.11.69.
[39] M. Finšgar, K. Xhanari, B. Petovar, A comparison of hydrochloric acid and acetate buffer media for trace metal analysis using Sb-film electrodes: a detailed electrochemical impedance spectroscopy study, J. Electrochem. Soc. 166 (2019) H108–H118, https://doi.org/10.1149/2.0191904jes.
[40] S. Christidi, A. Chrysostomou, A. Economou, C. Kokkinos, P.R. Fielden, S. J. Baldock, N.J. Goddard, Disposable injection molded conductive electrodes modified with antimony film for the electrochemical determination of trace Pb(II) and Cd(II), Sensors 19 (2019) 4809, https://doi.org/10.3390/s19214809.
[41] E.W. Nunes, M.K.L. Silva, I. Cesarino, Evaluation of a reduced graphene oxide-Sb nanoparticles electrochemical sensor for the detection of cadmium and lead in chamomile tea, Chemosensors 8 (2020) 53, https://doi.org/10.3390/chemosensors8030053.
[42] T. le Hai, L.C. Hung, T.T.B. Phuong, B.T.T. Ha, B.S. Nguyen, T.D. Hai, V.H. Nguyen, Multiwall carbon nanotube modified by antimony oxide (Sb_2O_3/MWCNTs) paste electrode for the simultaneous electrochemical detection of cadmium and lead ions, Microchem. J. 153 (2020), 104456, https://doi.org/10.1016/j.microc.2019.104456.